

## Some observations on no-load losses of an asymmetrical six-phase synchronous machine

Arif IQBAL\*, Girish Kumar SINGH, Vinay PANT

Department of Electrical Engineering, Indian Institute of Technology Roorkee, Roorkee, Uttarakhand, India

Received: 08.05.2015

Accepted/Published Online: 11.08.2015

Final Version: 20.06.2016

**Abstract:** The use of multiphase (more than three-phase) ac machines is well adopted in different high power applications and the evaluation of different losses (no load losses, short circuit load loss, friction and windage losses, and stray loss) in multiphase machines is extremely important for the correct determination of their operating performance. Therefore, the paper presents a detailed experimental investigation of an asymmetrical ( $30^\circ$  displacement between the two winding sets) six-phase synchronous machine for determination of different losses under no-load condition. Moreover, a comparative study of losses for a six-phase and three-phase synchronous machine has also been performed. The results are presented for different synchronous speeds (associated with frequency range 30–55 Hz).

**Key words:** Six-phase synchronous machine, no-load losses, multiphase machine

### 1. Introduction

The use of multiphase machines (both induction and synchronous) has been well adopted in various applications, because of several potential inherent advantages when compared with their three-phase counterpart. The important advantages are as follows [1–4]: reduction in torque pulsation, increased power handling capability, reduced per phase current without increase in voltage level, higher reliability etc.

Performance of any electrical machine, whether it is dc or ac (single phase, three-phase, or more than three-phase) is directly affected by the inherent presence of different losses (no load losses, short circuit load loss, friction and windage losses, and stray loss). In order to determine the accurate performance of electrical machines, determination of different losses is extremely important. A number of studies in the literature evaluated different losses of three-phase machines (both induction and synchronous), with standard test procedures [5,6]. References [7–10] deal with the losses in a six-phase induction machine and its comparison with its three-phase counterpart. However, no reference related to the detection of losses in a six-phase synchronous machine is available. Therefore, the main contribution of this paper is to present an experimental investigation for the determination of various losses under no-load condition in a six-phase synchronous machine. A comparative study of losses for a six- and three-phase synchronous machine has also been conducted.

### 2. Description of experimental setup

In order to evaluate the different losses, a 3.2-kW, 36-slot, 6-pole, 3-phase synchronous machine was used. On its terminal box, the end terminals of the stator winding coils were connected to realize the different winding scheme

\*Correspondence: arif.iqbal.in@gmail.com

for different numbers of phases and poles. Six-phase winding was obtained by using the technique of phase belt split [1,4] in a three-phase synchronous machine. The winding configuration of six phases was asymmetrical in nature, because of the existence of  $30^\circ$  electrical phase shift between the winding sets  $abc$  and  $xyz$ , having separate neutral points. Hence, fault propagation between the winding sets  $abc$  and  $xyz$  is prevented together with the prevention of flow of the third and its multiple harmonic current. Since the dc excitation system is an essential part of a synchronous machine, in the considered analytical and test system the synchronous alternator and excitation generator have been considered as a single entity. In the experimental setup, a 5-kW, 250-V, 21.6-A, 1372/1750-rpm dc machine (as motor) was mechanically coupled to the test machine. Measurement and recording of different experimental readings were carried out by using several analogue ammeters and voltmeters, together with the use of a power quality analyzer (Hioki 3197). A general view of the experimental setup is shown in Figure 1.

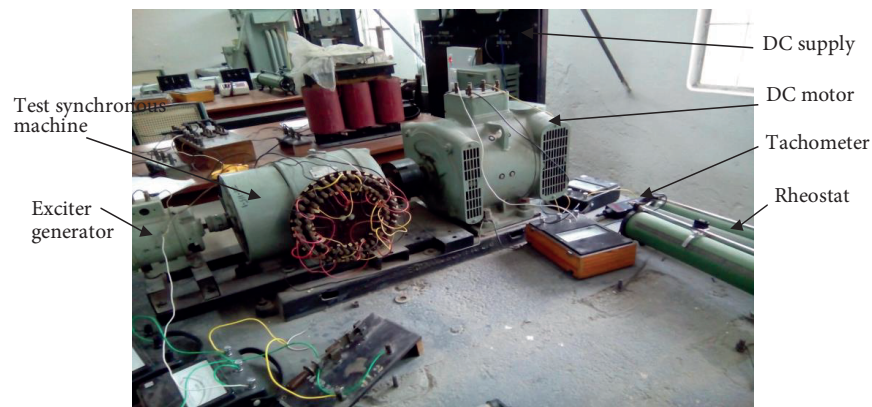


Figure 1. Experimental prototype showing complete setup.

### 3. Evaluation of fixed losses of DC machine

Initially, both machines (synchronous machine and dc machine) were mechanically uncoupled. The dc motor was run at the synchronous speed of the test machine, and current and voltage were recorded. Power input minus copper loss will give the iron loss, friction, and windage loss of the dc machine as given by

$$L_1 = V_a I_a - I_a^2 R_a, \quad (1)$$

where  $V_a$  and  $I_a$  are the input dc voltage and current fed to the dc motor, having its armature resistance  $R_a$ .

It is worthwhile to note here that the iron loss of the dc machine is dependent on both rotor speed and field current. At a constant speed, it becomes dependent on the flow of field current only. Therefore, at constant rotor speed, fixed losses,  $L_1$ , can be plotted as the function of motor field current,  $I_f$ . The results are presented in Figure 2, wherein the effects of both field current and rotor speed are shown. A series of experimental recording has been made at different speeds, i.e. at 600, 700, 800, 900, 1000, 1100 rpm (synchronous speed of 30, 35, 40, 45, 50, 55 Hz). Almost linear dependency of fixed losses may be noted not only on the motor field current but also on its rotor speed.

### 4. Determination of friction and windage losses

The test synchronous machine (acting as alternator) and its prime mover (i.e. dc motor) are mechanically coupled. The coupled machines are run at the synchronous speed with the field circuit of the test synchronous

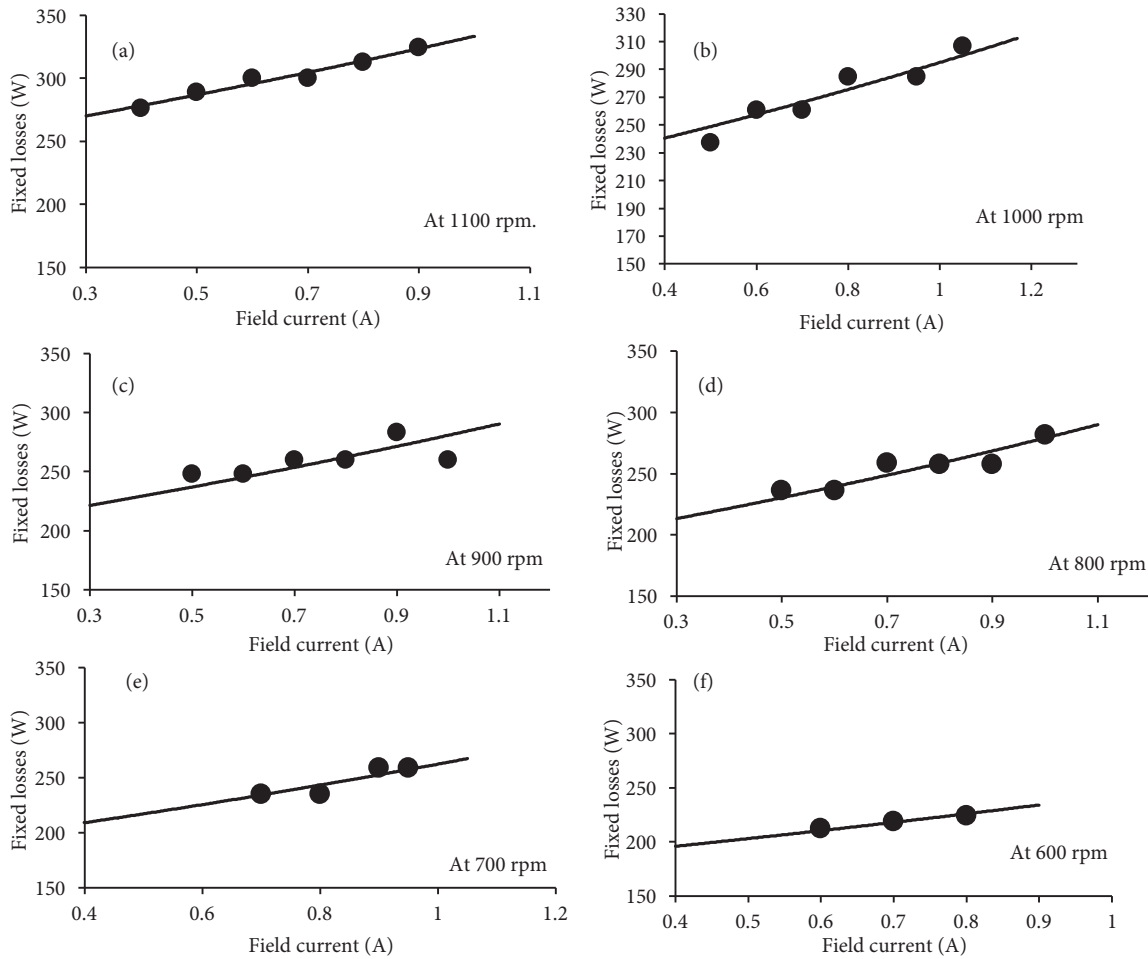


**Figure 2.** Fixed losses of dc motor at different rotor speed associated with the synchronous speed of (a) 1100 rpm, (b) 1000 rpm, (c) 900 rpm, (d) 800 rpm, (e) 700 rpm, (f) 600 rpm.

alternator remaining unexcited. During this condition, power taken by the dc motor will be equal to its losses ( $L_1 +$  armature copper loss) and windage and friction losses of the synchronous alternator ( $L_{fw}$ ). Mathematically,

$$L_{fw} = V_a I_a - I_a^2 R_a - L_1, \tag{2}$$

where the value of  $L_1$  (iron and friction and windage losses of the dc motor) is evaluated in an earlier section. This test was repeated for different rotor speeds, corresponding to different operating frequencies of the test synchronous alternator. An approximately linear dependency of friction and windage losses on rotor speed was noted, as depicted in Figure 3 by a green bar graph.

### 5. No-load losses in synchronous machine

DC supply is fed to the prime mover (dc motor) so as to run the alternator at synchronous speed. The field circuit of the alternator is excited with its armature open circuited. A series of readings was recorded for alternator generated voltage  $V_{oc}$ , dc motor field current  $I_f$ , input voltage  $V_a$ , and current  $I_a$  of the prime mover armature circuit, associated with different values of alternator field current  $I_{fr}$ . In this test, the input

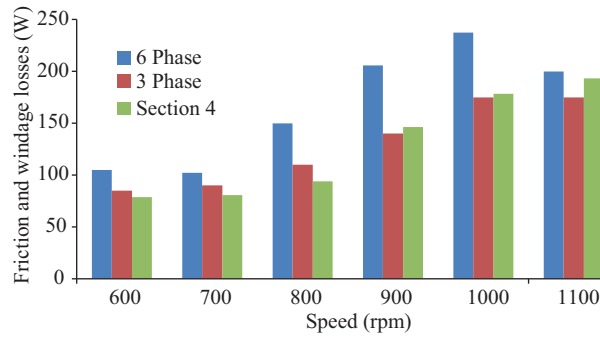


**Figure 3.** Friction and windage losses of synchronous machine by experiment in section 4 (green bar) and by experiment in section 5 for 6 phase (blue bar) and 3 phase (red bar).

power to the dc motor ( $V_a I_a$ ) basically accounts for different losses. These losses include the copper loss of motor armature circuit  $I_a^2 R_a$ , fixed losses of dc motor  $L_1$ , alternator friction and windage losses  $L_{fw}$ , and its core losses  $L_c$ . Mathematically, it can be expressed as

$$L_{fw} + L_c = V_a I_a - (L_1 + I_a^2 R_a). \tag{3}$$

It will be convenient to determine the value of  $(L_{fw} + L_c)$  graphically, with the variation in alternator generated voltage/field current. A series of experimental tests has been carried out on the test synchronous alternator having its winding configuration of both six phase as well as three phase, and the results are depicted in Figure 4. In general, the magnitude of no-load losses increases with the increase in generated open circuit voltage or field excitation current of the synchronous alternator at a particular rotor speed. Further, the magnitude of no-load losses increases with the increase in rotor speed, showing its dependency on the operating frequency. This magnitude was higher for the test synchronous alternator with its six-phase winding configuration. It is worthwhile to mention here that the  $y$ -intercept in Figure 4 determines the magnitude of friction and windage losses ( $L_{fw}$ ) of the test synchronous alternator, which are also shown in Figure 3. Friction and windage losses were found to be dependent not only on its operating rotor speed but also on the type of armature winding configuration (six- or three-phase stator winding of the test machine). In general, the value of  $L_{fw}$  is higher for the six-phase winding configuration when compared with its three-phase winding configuration of the test alternator. In addition to friction and windage losses, the major component of no-load losses is constituted by the core loss. This loss is inherently present in all electrical machines, dependent on the type of core material used, operating frequency, and flux level. The core loss consists of eddy current loss and hysteresis loss. A convenient way for the evaluation of these losses is discussed in the following section.

### 5.1. Separate evaluation of eddy and hysteresis losses

The component of machine core loss, i.e. eddy current loss ( $L_{ce}$ ) and hysteresis loss ( $L_{ch}$ ), are expressed as

$$L_c = L_{ce} + L_{ch} \tag{4}$$

$$L_{ce} = K_e f^2 B_m^2$$

$$L_{ch} = K_h f B_m^n, \tag{5}$$

where  $K_e$  = a constant, whose value depends on the type of ferromagnetic material used, lamination thickness, and volume of core material.

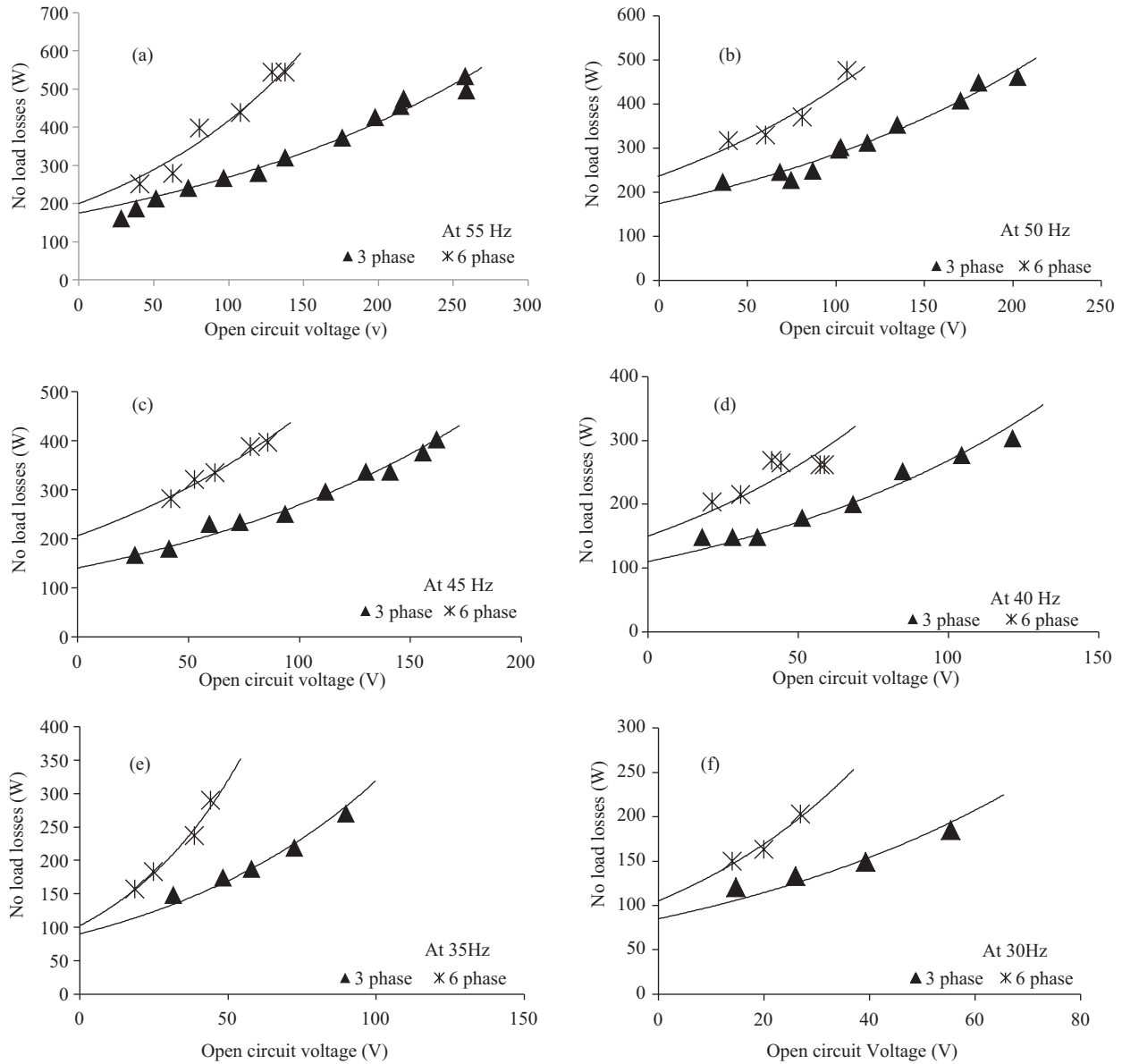


**Figure 4.** Experimental results of no-load loss of synchronous machine in 3-phase and 6-phase winding configuration at different synchronous speeds: (a) 55 Hz, (b) 50 Hz, (c) 45 Hz, (d) 40 Hz, (e) 35 Hz, (f) 30 Hz.

$K_h$  = a constant, whose value depends on core weight.

$B_m$  = maximum value of flux density.  $n$  denotes the Steinmetz constant, whose value varies from 1.5 to 2.5, depending on the magnetic properties of the core material.

Hence, eddy current loss varies with the squared value of frequency and hysteresis loss becomes proportional to the operating frequency at a fixed value of flux density (i.e. flux linkage of synchronous machine). Therefore, it will be convenient to rewrite Eq. (5) as

$$\begin{aligned} L_{ce} &= C_e f^2 \text{ (eddy current loss)} \\ L_{ch} &= C_h f \text{ (hysteresis loss)}. \end{aligned} \tag{6}$$

The values of constants  $C_e$  and  $C_h$  are determined experimentally for a fixed flux density. In this experiment,

the magnitude of test machine flux linkage is kept constant by just keeping the value of field excitation current at a fixed value. This is because the machine is operating at no-load condition with no-armature reaction, and flux linkage is determined by the field circuit only. Therefore, the field current of the alternator is kept constant at some suitable value, say 0.6 A, and a series of experimental data was recorded for different rotor speeds (synchronous speed corresponding to 30, 35, 40, 45, 50, 55 Hz). The results obtained are depicted in Figure 5 for both six-phase and three-phase winding configuration. In this figure, the expression for losses has been determined by curve fitting [11,12]. The constant term indicates the friction and windage losses; the first order term indicates the hysteresis loss, whereas the second order term indicates the eddy current loss. The hysteresis and eddy current losses are plotted for different operating rotor speeds/frequencies for both six-phase and three-phase winding configurations in Figure 6(a) and Figure 6(b), respectively. Clearly, both hysteresis and eddy current losses are greater in magnitude for the six-phase synchronous alternator than for its three-phase counterpart, resulting in the increased no-load losses in the six-phase synchronous machine. The reason behind this is explained below.

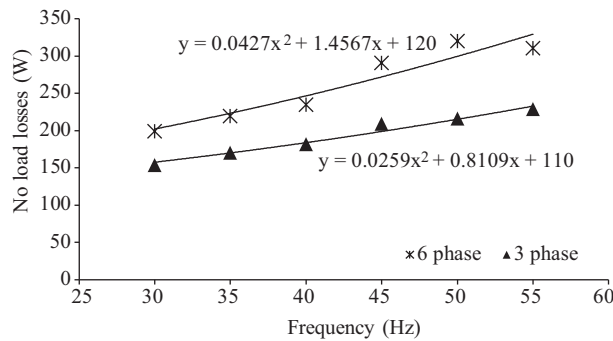


**Figure 5.** No load losses at constant flux density (field current at 0.6 A) of test machine under different synchronous speeds.

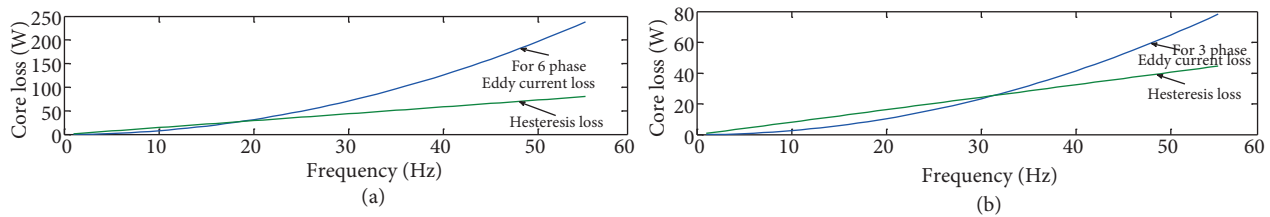


**Figure 6.** Separate evaluation of hysteresis loss and eddy current loss of test machine with its winding configuration of (a) six phase (b) three phase.

In the case of three-phase synchronous machine operation, there exists a magnetic interlocking between the stator and rotor field. Moreover, the salient structure of the rotor will align itself along the path of least reluctance. Therefore, during steady state, a small air gap,  $x$ , exists between rotor and stator field, as shown in Figure 7(a). However, during the machine operation with asymmetrical six-phase winding configuration, voltage is independently induced in both the winding sets  $abc$  and  $xyz$  of constant magnitude, while maintaining the phase shift of  $30^\circ$  electrical between the phase  $a$  and phase  $x$ . In this case, the rotor aligns itself along the resultant stator field as depicted in Figure 7(b). A rotor axis in this position will have the air gap  $x'$ , w.r.t. the magnetic axis of the individual winding sets  $abc$  and  $xyz$ . The air gap  $x'$  (for six-phase operation) is clearly greater than  $x$  (for three-phase operation). Therefore, to establish the required flux level in the air gap,

magnetizing current (i.e. field current  $I_{fr}$  in the present case) is increased, resulting in increased no-load losses in the test machine having asymmetrical six-phase winding configuration. Furthermore, in the machine with constant field excitation at no-load, flux linkage to stator winding with the three-phase configuration will be greater than its operation with six-phase winding configuration, because  $x' > x$ . Hence, voltage generation in the six-phase machine will be somewhat less than half the generated voltage (theoretically it should be exactly half) in armature winding in the three-phase configuration with increased no-load losses with the six-phase winding configuration.

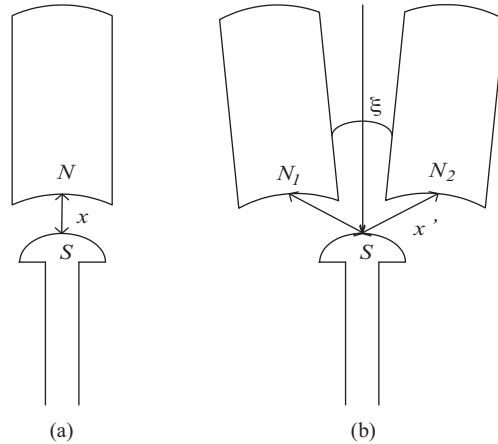


**Figure 7.** Effective air gap distance in machine operation for (a) three-phase operation and (b) six-phase operation.

**6. Determination of short circuit (SC) load test**

The rotor speed is maintained constant at synchronous speed from the prime mover side and the end terminals of the alternator stator winding is shorted (symmetrical SC). It should be noted that in the case of an alternator with the six-phase winding configuration, each three-phase set ( $abc$  and  $xyz$ ) is shorted separately. The power consumed by the dc motor ( $V_a I_a$ ) will be equal to the sum of losses  $L_1 + I_a^2 R_a + L_{fw}$ , together with the alternator load losses corresponding to the stator SC current. Hence, SC load loss can be easily evaluated by knowing the value of other losses from experiments 1, 2, and 3. Mathematically,

$$SC \text{ load loss} = V_a I_a - (L_1 + I_a^2 R_a + L_{fw}) \tag{7}$$

Further, stray load loss may be evaluated if the dc resistance of alternator stator winding  $r_1$  (and  $r_2$ ) is known, by using Eq. (8).

$$\text{Stray load loss} = (SC \text{ load loss}) - (\text{armature dc copper loss } I_{s1}^2 r_1 + I_{s2}^2 r_2), \tag{8}$$

where  $I_{s1}$ ,  $I_{s2}$  and  $r_1$ ,  $r_2$  are the stator phase current and dc resistance of both winding sets  $abc$  and  $xyz$ , respectively.

These experimental steps have been carried out for both six-phase and three-phase stator winding configuration at different rotor speeds. At a particular stator winding configuration, the SC loss magnitude was found to be dependent on the flow of stator current only and not much affected by rotor speed for particular field excitation. This is depicted in Figure 8, wherein the dependency of SC loss on the squared value of stator current is signified by the straight line. The SC load loss comprises the armature copper loss, core loss due

to armature leakage flux, and a small core loss due to resultant flux. Magnitude of the stator current is much larger in the six-phase winding configuration than in its three-phase counterpart. However, the magnitude of total armature copper is almost the same for both six-phase and three-phase winding. In the case of six-phase operation, on the other hand, magnitude of leakage flux and also the resultant flux are increased. The increased magnitude of flux linkage results in higher magnitude of core loss. Therefore, the magnitude of SC loss was found to be higher with the six-phase stator winding configuration than with its three-phase counterpart. By utilizing the evaluated values of SC loss, Eq. (8) was used to find the alternator stray loss. This is expressed for stator current of 2 A at different rotor speeds for both six-phase and three-phase winding configuration as shown in Figure 9. Stray loss was also found to be greater for the six-phase winding configuration than for its three-phase counterpart.

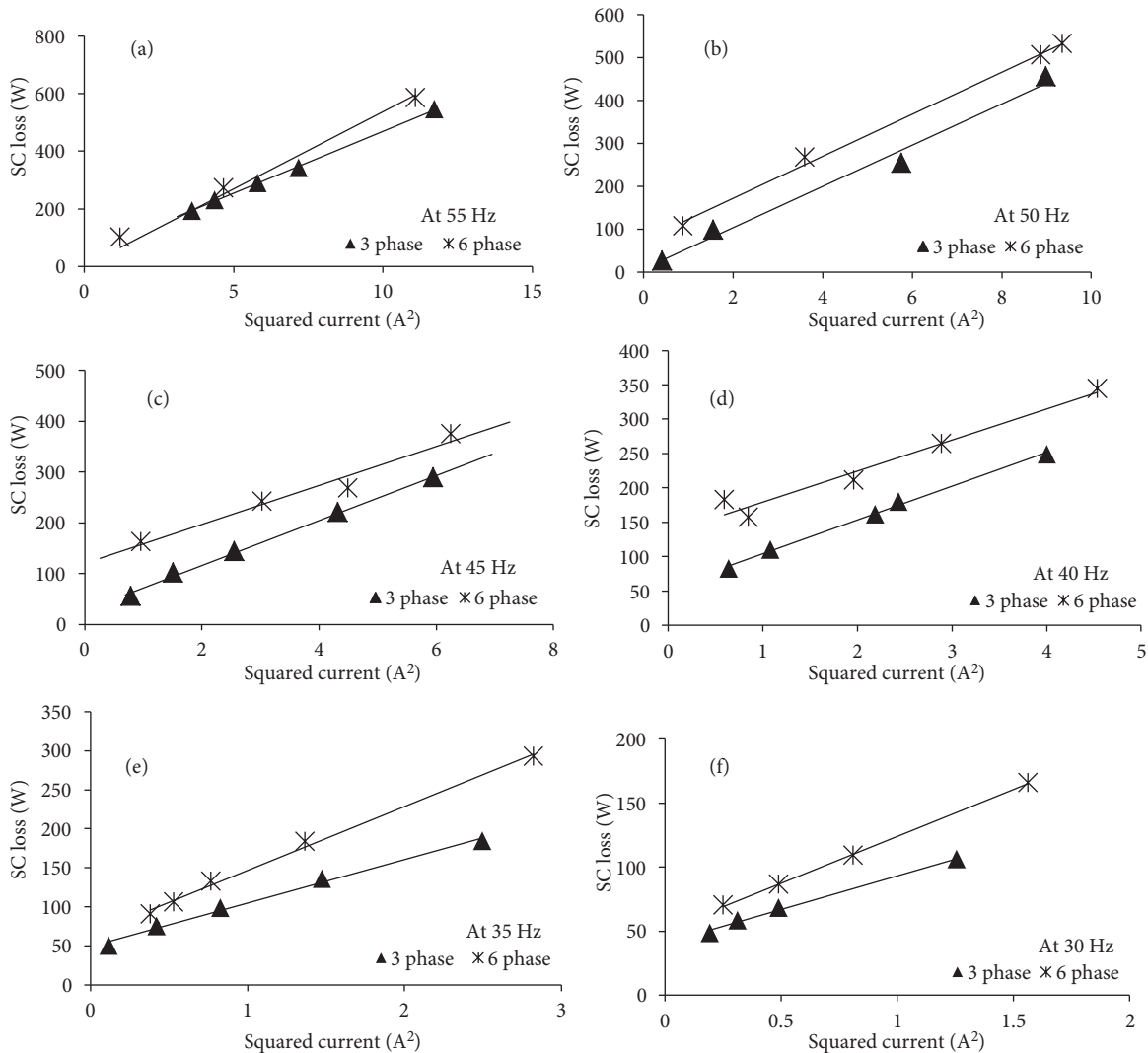


**Figure 8.** Short circuit loss of test synchronous machine at different rotor speeds.

During the process of loss determination, the existence of its small irregular trend may also be noted. This is because of continuous variation in loads connected to the utility grid, resulting in change in input (dc through rectifier) voltage. During the experiment, rotor speed was also controlled manually by using a rheostat



in the armature and field circuit of the prime mover. It is time consuming and practically difficult to maintain the rotor speed exactly constant. These factors, together with the manual recording of a larger number of measuring devices, may result in some error.

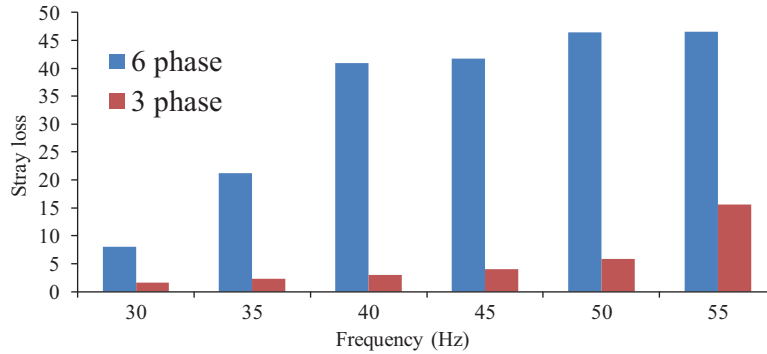


Figure 9. Stray loss at different synchronous speeds.

### 7. Determination of field circuit losses (copper loss)

Determination of field copper loss requires an accurate value of field circuit resistance. Since the value of resistance is dependent on the operating temperature, the corrected value of resistance may be obtained by using Eq. (9).

$$R_1 = R_2 \frac{(k + t_1)}{(k + t_2)}, \tag{9}$$

where  $R_1$  and  $R_2$  are the resistance at cold standard temperature  $t_1$  such as 25 °C and at operating condition temperature  $t_2$ .  $K$  is a constant whose value depends on the type of material used. Furthermore, the value of brush resistance loss will also have to be taken into consideration. This value at an individual slip ring is equal to the product of (field current  $\times$  1 volt drop) watts. Alternatively, the field circuit copper loss may be evaluated if the magnitude of brush voltage  $V_{fr}$  is known for a given value of field current  $I_{fr}$ . The value of field current should maintain the rated terminal voltage of the synchronous alternator at a particular operating condition.

In the experimental setup, a small exciter generator is mounted to feed the field circuit through the slip ring and brush arrangement. The magnitude of generated voltage is proportional to the shaft speed. Using the generated voltage together with the above-discussed experimental steps, copper loss of the field circuit may be determined at different excitation currents ( $I_{fr}$ ), as shown in Figure 10.

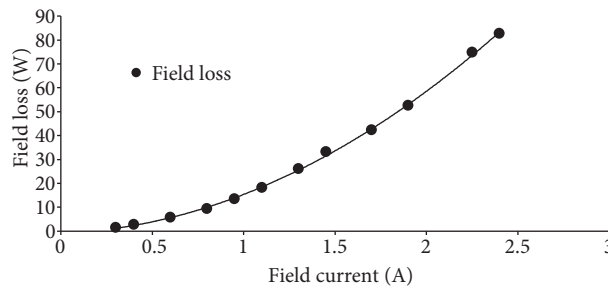


Figure 10. Field loss in excitation circuit.

## 8. Conclusion

This paper presents a detailed experimental evaluation of different losses of a six-phase synchronous machine. Results have been presented for different rotor synchronous speeds (at frequency of 30, 35, 40, 45, 50, 55 Hz). In general, the different no-load losses of the synchronous machine with six-phase winding configuration were found to be greater than those of its three-phase counterpart. Some of the important concluding remarks may be listed as follows:

- (a) Friction and windage losses were a linear function of rotor speed.
- (b) No-load losses of the test synchronous machine were dependent on both field voltage/current and rotor speed. At a particular excitation, the difference in no-load losses for the machines with six-phase and three-phase winding configuration increases linearly with rotor synchronous speed. Furthermore, increased no-load loss (resulting in increased core loss) for the six-phase operation is due to the increased effective air gap  $x$  between the rotor and stator magnetic axis of individual winding sets ( $abc$  and  $xyz$ ).
- (c) In the six-phase test machine, the magnitude of short circuit loss is higher than that of its three-phase counterpart. This is mainly because of the increased magnitude of resultant flux, thereby increasing the value of local core losses.
- (d) Losses in the field circuit are dependent on the magnitude of its excitation current. These losses are independent of the rotor speed at a particular excitation current. Losses in the field circuit were found to be proportional to the squared value of excitation current.

The different no-load loss components of the synchronous machine with the six-phase winding configuration were greater than those of its three-phase counterpart. However, during load condition, the per phase current in the six-phase winding configuration is substantially reduced for a given load. Further, the asymmetrical six-phase winding configuration with displacement angle of  $30^\circ$  electrical results in the elimination of all the air gap flux harmonics of order  $(6x \pm 1; x = 1, 3, 5 \dots)$ . This leads to a substantial decrease in losses (particularly stray loss) and overall improved performance of the six-phase synchronous machine as compared to its three-phase counterpart.

## References

- [1] Singh GK. Multiphase induction machine drive research - a survey. *Elect Pow Syst Res* 2002; 61: 139-147.
- [2] Levi E. Multiphase electric machines for variable-speed applications. *IEEE T Ind Electron* 2008; 55: 1893-1909.
- [3] Singh GK. Modeling and analysis of six-phase synchronous generator for stand-alone renewable energy generation. *Energy* 2011; 36: 5621-5631.
- [4] Klingshrin EA. High phase order induction motor - part-I: description and theoretical consideration. *IEEE T Power Ap Syst* 1983; 102: 47-53.
- [5] Kohli DR, Jain SK. *A Laboratory Course in Electrical Machines*. 2nd edition, India: JBA Publisher, 2000, pp. 300-307.
- [6] The Institute of Electrical and Electronics Engineers Inc. 1995 IEEE Guide: Test Procedures for Synchronous Machines (IEEE Std 115-1995).
- [7] Klingshrin EA. High phase order induction motor - part-II: experimental results. *IEEE T Power Ap Syst* 1983; 102: 54-59.

- [8] Boglietti A, Bojoi R, Cavagnino A, Tenconi A. Efficiency analysis of PWM inverter fed three-phase and dual three-phase high frequency induction machines for low/medium power applications. *IEEE T Ind Electron*; 2008; 55: 2015-2023.
- [9] Dorrell DG, Leong CY, McMahon RA. Performance assessment of six-pulse inverter-fed three phase and six phase induction machine. *IEEE T Ind Appl* 2006; 42: 1487-1495.
- [10] Singh GK. A six-phase synchronous generator for stand-alone renewable energy generation: experimental analysis. *Energy* 2011; 36: 1768-1775.
- [11] Lancaster P, Salkauskas K. *Curve and Surface Fitting: An Introduction*. San Diego, CA, USA: Academic Press, 1990.
- [12] Guest PG. *Numerical Method of Curve Fitting*. New York, NY, USA: Cambridge University Press, 2013.